Vol. 726: 31–47, 2024
https://doi.org/10.3354/meps14485

MARINE ECOLOGY PROGRESS SERIES
Mar Ecol Prog Ser

Published January 11

Size-fractioned zooplankton biomass in the Barents Sea: macroecological patterns across biogeography, climate, and varying ecosystem state (1989–2020)

Hein Rune Skjoldal[1,*], Erik Sperfeld[2]

[1]Institute of Marine Research, Bergen 5005, Norway
[2]Animal Ecology, Zoological Institute and Museum, University of Greifswald, Greifswald 17489, Germany

ABSTRACT: The zooplankton community in the Barents Sea was monitored during autumn cruises from 1989–2020, with biomass determined as the depth-integrated dry weight (g m^{-2}) of 3 size fractions (>2 mm, 1–2 mm, <1 mm). A large data set of 4543 sampling stations encompassing a subdivision of the Barents Sea was spatially averaged into 15 polygons based on topography. The resulting data set is used to describe relationships between the biomass of size fractions as expressions of the size structure of the zooplankton communities. Each of the 3 size fractions was positively related to the total zooplankton biomass (sum of fractions). The medium size fraction, which contained on average 48% of the total biomass, showed a strong linear correlation with total biomass ($R^2 \approx 0.8$). The medium fraction contained the older copepodite stages of *Calanus* species (*C. finmarchicus* and *C. glacialis*), which are dominant species interpreted to drive the overall changes in zooplankton biomass. The biomass of the small size fraction decreased with decreasing total biomass, but less so than the medium fraction. Thus, the small/medium biomass ratio increased as the total biomass decreased. This trend was most pronounced for shallow and central polygons, which coincide with the core feeding area of the large Barents Sea stock of capelin *Mallotus villosus*. The change in the small/medium biomass ratio is interpreted to reflect a shift from *Calanus* to smaller zooplankton in response to predation by capelin and other planktivorous predators, and possibly also by warming due to climate change.

KEY WORDS: *Calanus* · Capelin · Climate change · Fish predation · Marine ecosystem · Plankton dynamics · Size fractions · Zooplankton biomass

1. INTRODUCTION

Zooplankton serves as the intermediate link between phytoplankton primary production and higher trophic level consumers in marine ecosystems. Zooplankton represents a complex of many species from a variety of different taxonomic groups, spanning a wide range in body size and trophic types. Mesozooplankton is commonly defined as small pelagic animals in the size range of 0.2–20 mm (Lenz 2000); copepods are the main group of species making up the mesozooplankton in marine ecosystems, especially in colder waters at high latitudes (Longhurst 1985). Large calanoid copepods are especially important at high latitudes, with prominence of *Calanus* and *Neocalanus* species in northern boreal, subarctic, and Arctic waters (Conover 1988). 'Large' is used here in a relative sense; these copepods are still small organisms around 3–10 mm in length, but large enough to be able to survive the long dark winter with little or no primary production, using energy from stored lipid body reserves (Conover & Huntley 1991).

The 2 sibling species *Calanus finmarchicus* and *C. glacialis* are the dominant copepods in the Barents Sea (Tande 1991, Melle & Skjoldal 1998, Falk-Petersen et al. 2009). *C. finmarchicus* is a boreal basin

*Corresponding author: hein.rune.skjoldal@hi.no

Publisher: Inter-Research · www.int-res.com

species in the North Atlantic with core distribution areas in the Norwegian and Labrador seas (Marshall & Orr 1955, Helaouët et al. 2011, Melle et al. 2014). *C. glacialis* is an Arctic species found predominantly in subarctic shelf seas with seasonal ice cover around the periphery of the Arctic Ocean (Conover 1988, Weydmann et al. 2016). *C. finmarchicus* has predominantly a 1 yr life cycle in the boreal, Atlantic water of the southern Barents Sea (Tande 1991, Melle & Skjoldal 1998), although it may produce 2 generations in the warmer inflowing Atlantic water (Strand et al. 2020, Skjoldal et al. 2021). *C. glacialis* is found in the colder Arctic water of the northern Barents Sea, where it may have a 2 yr life cycle to complete its generational development (Tande 1991, Melle & Skjoldal 1998, Daase et al. 2013). The 2 *Calanus* species make up most of the biomass of mesozooplankton in the Barents Sea, estimated to be on average 70–80%, with a dominance of *C. finmarchicus* in the south and *C. glacialis* in the north (Aarflot et al. 2018).

Zooplankton has been monitored in the Barents Sea in a joint program between Norway and Russia since the 1980s (Orlova et al. 2011). The Institute of Marine Research (IMR) in Norway uses a procedure to determine zooplankton biomass in 3 size fractions following wet sieving with 2- and 1-mm screens (large, medium, and small fractions: >2 mm, 1–2 mm, and <1 mm, respectively) (Melle et al. 2004, Skjoldal et al. 2013). Large-scale monitoring is carried out in autumn (mid-August–early October), towards the end of the productive period and of the seasonal development of the cohorts of *Calanus* species, which become the overwintering generations. The size fractionation separates small copepods (including *Pseudocalanus*, *Microcalanus*, and *Oithona*) in the small size fraction from the older and biomass-dominant copepodite stages of the *Calanus* species found in the medium size fraction (Skjoldal 2021).

The Barents Sea is a high-latitude ecosystem located between approximately 70° and 80° N (see Fig. 1). It consists of a biogeographic transition between the boreal south and Arctic north, and is home to large commercial fish stocks and large numbers of seabirds and marine mammals (Wassmann et al. 2006, Jakobsen & Ozhigin 2011, Hunt et al. 2013). The Barents Sea stock of Atlantic cod *Gadus morhua* is the largest in the world (Kjesbu et al. 2014). The Barents Sea is a nursery area for the largest stock of Atlantic herring *Clupea harengus* (the Norwegian spring spawning stock) and is home to large stocks of Atlantic capelin *Mallotus villosus* and polar cod *Boreogadus saida*. The capelin stock overwinters in the central Barents Sea and migrates seasonally on a feeding migration into the cold Arctic waters of the northern Barents Sea, where they feed on *C. glacialis* and other prey (Sakshaug & Skjoldal 1989, Skjoldal & Rey 1989, Giske et al. 1998). Juvenile herring feed on *C. finmarchicus* and other prey in the southern Barents Sea (Krysov & Røttingen 2011), whereas polar cod forage mainly in the cold waters of the eastern and northern Barents Sea (Hop & Gjøsæter 2013). These 3 main planktivorous fishes have broadly divided the Barents Sea among them (herring in the south, capelin in the central-north, and polar cod in the east and north; Eriksen et al. 2017).

The Barents Sea ecosystem has undergone substantial changes in recent decades. It has experienced a strong warming of nearly 2°C since 1980 (Skagseth et al. 2020), with an associated marked increase in primary production (Dalpadado et al. 2020). The capelin stock has shown strong fluctuations, with 4 collapses followed by rapid recoveries in broadly a decadal pattern since 1980 (Gjøsæter et al. 2009, Berg et al. 2021, Skjoldal 2023). The stock of Atlantic cod has increased and expanded northward in response to the general warming, driven by a combination of favorable recruitment conditions and good management practices (Kjesbu et al. 2014, Johannesen et al. 2020). Many other fish species have expanded their distribution northward in the Barents Sea in a process called 'borealization' associated with ongoing 'Atlantification' (Fossheim et al. 2015, Kortsch et al. 2015, Frainer et al. 2017, Ingvaldsen et al. 2021). Increased abundance and geographical expansion have also been seen for krill species among macrozooplankton (Eriksen et al. 2016, 2017, Stige et al. 2019).

The size-fractioned zooplankton biomass data from the IMR monitoring program were examined in relation to climate and predation by planktivorous fish by Stige et al. (2014), using data up to 2010. Their study found inverse relationships between the biomass of the medium and large fractions on the one hand, and the biomass of the Barents Sea capelin stock and temperature of the Atlantic water on the other. Patterns of spatial and temporal variations were examined recently with an extended data set up to 2020, using a spatial division of the Barents Sea into 15 subareas or polygons (see Fig. 1) (Skjoldal et al. 2022b). This study confirmed the inverse relationships between zooplankton biomass and capelin stock size and temperature, interpreted to reflect the combined effects of predation and climate warming. A prominent spatial pattern in the last 2 decades has been an increase in zooplankton in the inflowing Atlantic water in the southwest and a decrease in zooplankton biomass in the central part of the Barents Sea (Skjoldal 2023).

This is interpreted to reflect a second summer generation of *C. finmarchicus* in the Atlantic water (Skjoldal et al. 2021) and a decline of *C. glacialis* in the central area due to less sea ice and increased predation from capelin in a prolonged feeding season that provides sufficient light for predation (Langbehn & Varpe 2017, Skjoldal et al. 2022b).

Here, we report zooplankton biomass of the 3 size fractions for the 1989–2020 period, expressed as mean values for the polygons of the Barents Sea during the annual autumn surveys. We explore the relationships among the 3 fractions as broad expressions of changes in the size structure of the Barents Sea zooplankton in relation to spatial and temporal variations. Skjoldal et al. (2022b) described interannual and spatial patterns of the zooplankton biomass data and reported a positive relationship between the ratio of the small to medium size fractions and the size of the capelin stock, believed to reflect a shift from *Calanus* to smaller zooplankton due to fish predation. Here, we build on this previous study while conducting our analysis at the macroecological level, revealing patterns and trends in the relationships of size fractions across the entire data set. This analysis includes effects from biogeography ranging from the boreal to the Arctic domains, effects from climate warming over more than 3 decades, and effects from the many biological and ecological changes in the ecosystem associated with biogeography, climate change, and shifting ecosystem dynamics. We also examine patterns among the zooplankton fractions with a subdivision of the data set along 3 dimensions: depth (comparing shallow and deep polygons), geography (comparing southern, central, and northern polygons), and time (comparing an early and late period).

At this macroecological level at the scale of a large marine ecosystem, the closest we come to a hypothesis is that we expect warming and increased predation from planktivorous fish to cause a shift towards smaller forms of zooplankton. Planktivorous fishes such as capelin and herring select larger individuals of zooplankton (e.g. large *Calanus*) while they discriminate against small individuals (e.g. small copepods) due to low visibility and low capture efficiency (Aksnes & Giske 1993). Large body size is a competitive advantage for large calanoid copepods, allowing them to survive the long winter at high latitudes. A warmer climate may reduce this advantage, especially in combination with loss of sea ice, which makes large forms more vulnerable to predation from visual predators such as capelin and polar cod (Langbehn & Varpe 2017, Langbehn et al. 2023).

2. MATERIALS AND METHODS

2.1. Sampling and determination of biomass

Zooplankton was sampled during joint Norwegian–Russian cruises in the Barents Sea in autumn from mid-August to early October each year (Eriksen et al. 2018). Samples, usually from 3 Norwegian (IMR) research vessels in the annual semi-synoptic surveys, were obtained with vertical hauls from near the bottom (ca. 10 m above) to the surface with WP2 plankton net (0.25 m^2 opening and 180 µm mesh size; Skjoldal et al. 2019). Each sample was processed with a standard method involving splitting the sample into 2 halves for the determination of biomass and preservation (with formaldehyde) for taxonomic analyses, respectively (Hassel et al. 2020).

Biomass is determined as dry weight after successive wet-sieving through 2 mm, 1 mm, and 180 µm screens. Zooplankton organisms retained on the 3 screens are weighed separately, following transfer to pre-weighed aluminum trays and drying at 65°C for 24 h or more. The 3 fractions are denoted large (>2 mm), medium (1–2 mm), and small (<1 mm), and total zooplankton biomass is derived as the sum of the 3 fractions. The stated size limits are the mesh sizes of the screens, but they have been found to be related to the size of copepods (and cladocerans) in a strict and predictable manner (Skjoldal 2021). Small copepods (<0.4 mm in prosome width), including *Pseudocalanus*, *Microcalanus*, *Oithona*, and young copepodite stages (CI–CIII) of *Calanus finmarchicus* and *C. glacialis*, are contained in the small fraction. The 1 mm screen has a separation curve where it starts to retain copepods at a width of 0.4 mm and retains most of the copepods at a width of 0.8 mm. The medium fraction contains the biomass-dominant older copepodite stage CV and adults of *C. finmarchicus* and *C. glacialis*, while stage CIV of these copepods is split about 50–50 in the small and medium fractions. Small invertebrate larvae (polychaetes, bivalves, gastropods) and appendicularians are found mainly in the small fraction, whereas larger individuals of chaetognaths, copepods (*Paraeuchaeta*, *C. hyperboreus*), krill, and amphipods are found in the large fraction (Skjoldal 2021).

2.2. Data set

The data set of samples from autumn cruises during 1989 to 2020 comprised a total of 4543 stations with one vertical WP2 net haul at each station. The stations were sorted by 15 subareas or polygons (Fig. 1),

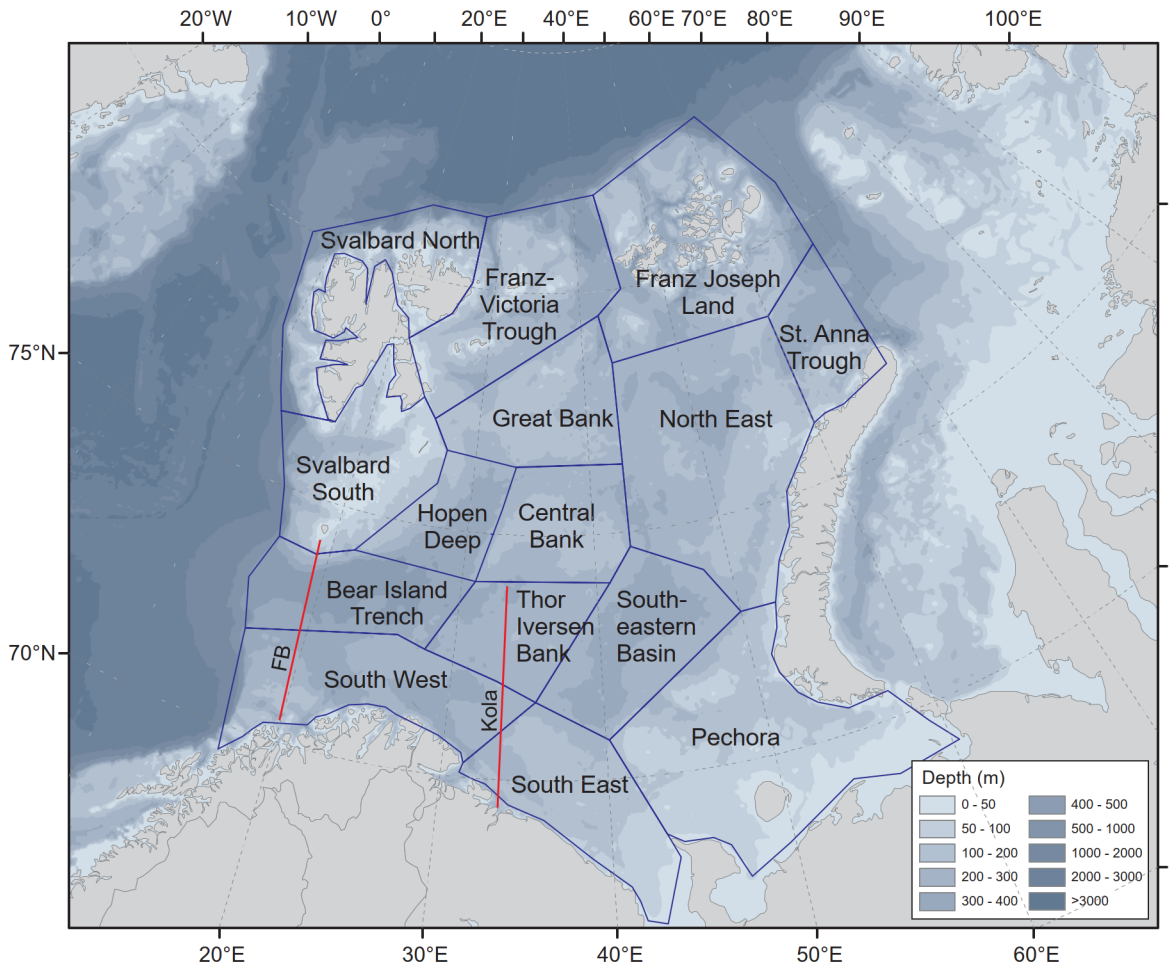

Fig. 1. Barents Sea, showing bottom topography and subdivision into 15 polygons (Dalpadado et al. 2020). Red lines: standard oceanographic transects used to monitor climate: FB (Fugløya-Bear Island section) and Kola section (Ingvaldsen et al. 2021)

and annual mean autumn biomass values for the 3 size fractions and their sum (total biomass) for each of the polygons were calculated. Most of the samples (~90%) were obtained from 9 polygons in the western and central Barents Sea. An overview of the samples as well as all polygon results (mean and SD for annual values) are given in Skjoldal et al. (2022b). We have excluded polygon mean values based on only one or 2 stations (24 and 14 cases for a total of 52 stations) due to relatively large uncertainty associated with low sample size. Excluding additional stations with missing values brought the number of annual polygon mean values of the present data set to 304, based on a total number of 4469 stations with an overall average of 15 stations per annual polygon mean biomass value. The associated coefficients of variation (CV = SD / mean) for the annual mean polygon biomass values were 1.11, 0.82, 0.58, and 0.61 for the large, medium, and small fractions, and total biomass, respectively (Skjoldal et al. 2022b).

2.3. Data analysis

Depth-integrated biomass is presented as g dry weight (DW) m^{-2}. We used $\log_{10}$ transformation of the data for regression and other analyses. Plots of linear data showed scatter of data points at the high end of the scale (Fig. S1 in the Supplement at www.int-res.com/articles/suppl/m726p031_supp.pdf). Log-transformed data were more balanced and closer to a normal distribution but revealed some scatter at the low end of the scale (Fig. S1). We believe this reflects a larger relative error in determining low biomass values in combination with inflation of the low end of the log scale. Due to the disproportionately large influence of the scattered low data points, we ran regressions with both the full data set and data excluding the low values.

We used ordinary linear regression (OLR) to investigate the relationship between the log-transformed biomass of each of the 3 fractions and the total zoo-

plankton biomass. Regressions were run in R version 4.1.2 (R Core Team 2021); output included regression plots with a 95% confidence band for the regression line and regression slopes with 95% confidence intervals (CIs). Statistical significance of differences in regression slopes was indicated by non-overlapping CIs.

Since the total zooplankton biomass is the sum of the 3 fractions, regressing each of the fractions against the total biomass violates the principle of statistical independence between the 2 regressed variables. This may contribute to a positive correlation between the two. The variation in biomass of a fraction can be separated into real variation due to space (polygons) and time (years), and a random component reflecting error in measurements. Relatively low variance in biomass data obtained with the same size-fractionation procedure for repeated replicate sampling suggested that the measurement error associated with processing samples was generally low (Skjoldal et al. 2013). In our case, any random error in measurements is further reduced by the use of means for polygons based on an average of 15 stations. We used OLR to compare the slopes of the (positive) relationships to explore shifts in the relative importance of the different fractions along the total biomass gradient.

The ratio of biomass of the small to medium size fractions was used to indicate changes in the size distribution of the mesozooplankton assemblages. The small to medium ratio was calculated for each set of mean values for polygons (n = 304) and regressed against total zooplankton biomass (both $\log_{10}$ transformed).

The total data set of mean values for polygons was divided into 2 or 3 portions according to time (years), depth, and geographical regions. For time, the data set was divided into early (1989–2006) and late (2007–2020) periods, based on a decrease in the large fraction around 2006–2007 (see Skjoldal et al. 2022b). With respect to depth, the data set was split into 2 groups of shallow (<220 m; Central Bank, Great Bank, Svalbard South, South East, North East, and Pechora) and deep (>255 m; Bear Island Trench, Thor Iversen Bank, Hopen Deep, South West, Southeastern Basin, and Svalbard North) polygons (see Fig. 1 for polygon locations). With respect to geography (and biogeography), the data set was split into 3 groups of polygons: southern/Atlantic (South-West, Bear Island Trench, and Thor Iversen Bank), central/core capelin area (Central Bank, Great Bank, and Hopen Deep), and northern/Arctic (Franz-Victoria Trough, North-East, and Svalbard-North). Regressions were run separately for the subsets of data, similar to the analyses for the total data set described above but for the version excluding the low biomass values showing high scatter in the low end of the range.

The statistical significance of differences between mean biomass values for the split data sets was tested with *t*-tests for comparisons between 2 groups (shallow vs. deep polygons and early vs. late periods), with Tukey's HSD post hoc test following 1-way ANOVA for pairwise comparisons among 3 groups (Atlantic, Central, and Arctic polygons) (R Core Team 2021).

3. RESULTS

3.1. Statistical properties of data

The large, medium, and small size fractions made up on average 16, 48, and 35% of the total biomass across all mean values for polygons (Table 1). The relative variation, expressed as CV, was similar for the small and medium fractions (0.57 and 0.58), while being somewhat larger (0.71) for the large fraction. The variation was lower for the total (sum of fractions), with a CV of 0.47 (Table 1). The median values were less than the means (from 5% [total] to 15% [large]; Table 1), indicating some deviation from a symmetrical distribution for linear (untransformed) data. Values of kurtosis and skewness likewise suggested moderate deviation from normal distributions, with values in most cases <3 (Table 1). Lower median than mean and positive skewness values demonstrate left-leaning distributions with a tail in the high end.

Following log transformation, the data were closer to a normal distribution (log normal), suggested by

Table 1. Summary statistics for zooplankton biomass (g DW m^{-2}) in 3 size fractions and total, based on annual mean biomass values (autumn) for polygon areas (untransformed data) in the Barents Sea. Kurtosis and skewness are also given for $\log_{10}$-transformed data

	Large	Medium	Small	Total
Mean	1.18	3.49	2.55	7.23
%	16.3	48.4	35.4	100
SD	0.84	2.02	1.46	3.39
CV	0.71	0.58	0.57	0.47
Median	0.99	3.22	2.25	6.90
Minimum	0.03	0.19	0.22	0.75
Maximum	4.96	12.54	10.37	23.18
Kurtosis	2.19	2.71	9.71	3.23
Skewness	1.28	1.25	2.49	1.24
Kurtosis log	0.93	1.75	1.99	1.43
Skewness log	−0.83	−0.96	−0.31	−0.70
n	304	304	304	304

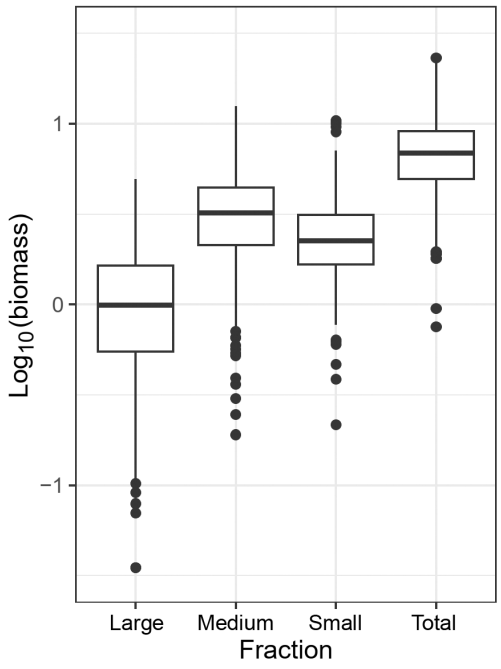

Fig. 2. Box–whisker plots of zooplankton biomass (g DW m^{-2}) of different size fractions (large: >2 mm; medium: 1–2 mm; small: <1 mm) and total (sum of fractions) for the full data set of 304 polygon mean values. The plots show median values (horizontal bar), 25 and 75 percentiles (box), 5 and 95 percentiles (vertical lines), and statistical outliers (points). Data are log_{10} transformed

lower values of kurtosis and skewness (<2; Table 1). Box–whisker plots of the frequency distributions of log-transformed data revealed balanced distributions around the median values but with some statistical outliers in the low end of the range for each of the 3 fractions (Fig. 2). Reflecting this scatter in the low end of the distributions (Fig. S1), skewness was negative although with small values close to zero (between −0.3 and −1.0; Table 1).

Frequency distributions of biomass of the 3 size fractions as proportions of total biomass demonstrate normal-like distributions, with the largest discrepancy for the small fraction (Fig. S2 in the Supplement). Ranges of the proportions over all samples were 0–57% for the large fraction, 7–80% for the medium fraction, and 8–87% for the small fraction.

Table 2. Correlation coefficients (Pearson product-moment r) for the variation among the 3 size fractions of zooplankton and for the variation in each fraction versus total biomass (sum of the fractions) across the data set of polygon means (n = 304). Correlations are based on log_{10}-transformed data

	Large	Medium	Small
Medium	0.52		
Small	0.27	0.46	
Total	0.64	0.90	0.73

3.2. Correlations among fractions

The 3 size fractions were positively correlated over the data set of polygon means, with the highest correlation for the medium fraction versus the large and the lowest correlation for the small fraction versus the large (Table 2). Correlations for each of the 3 fractions versus total biomass (sum of the 3 fractions) were higher, with R^2 values of 0.81, 0.53, and 0.41 for the medium, small, and large fractions, respectively (Table 2).

3.3. Regression analysis of biomass of fractions versus total biomass

3.3.1. Total data set

Linear regressions of biomass of each of the 3 fractions versus total biomass (sum of the 3 fractions) showed positive and statistically significant relationships, with each fraction contributing positively to the total biomass (Fig. 3, Table 3). There was more scatter

Table 3. Results of regressions between zooplankton biomass (g DW m^{-2}) of 3 size fractions (small: <1 mm; medium: 1–2 mm; large: >2 mm) versus total zooplankton biomass. Log_{10}-transformed data were used in the regression analyses. Regressions were calculated using the full data sets (F; i.e. based on both the black and grey data points shown in Fig. 3), and restricted (R) data sets excluding low values (i.e. based only on the black data points). The R regressions are shown in Fig. 3

Regression	n	Intercept	Slope	95% CI (slope)	SE (slope)	*t* (slope)	p (slope)	R^2
Small (F)	304	−0.263	0.757	0.677–0.838	0.041	18.6	<0.001	0.53
Small (R)	296	−0.196	0.687	0.607–0.768	0.041	16.9	<0.001	0.49
Medium (F)	304	−0.505	1.196	1.131–1.261	0.033	36.4	<0.001	0.81
Medium (R)	299	−0.468	1.157	1.097–1.218	0.031	37.5	<0.001	0.83
Large (F)	304	−0.941	1.092	0.945–1.240	0.075	14.6	<0.001	0.41
Large (R)	292	−0.829	0.982	0.835–1.129	0.075	13.1	<0.001	0.37

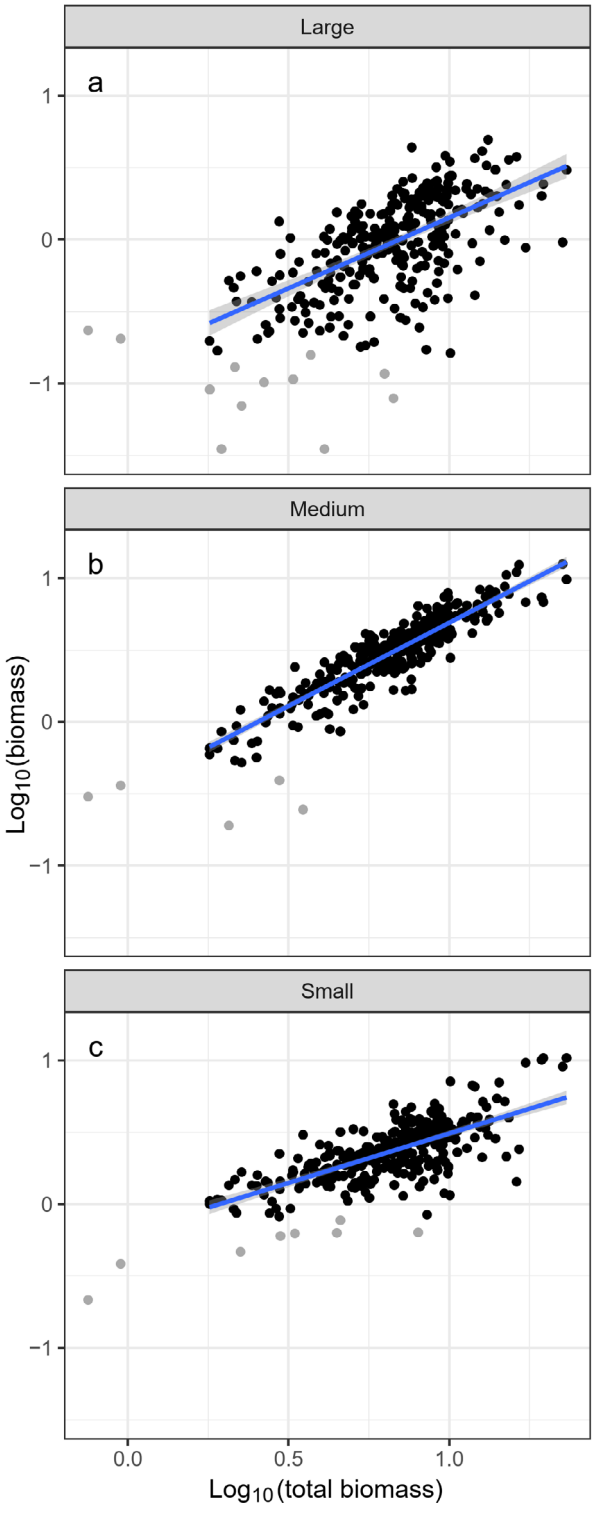

Fig. 3. Relationship between zooplankton biomass (g DW m^{-2}) of (a) large (>2 mm), (b) medium (1–2 mm), and (c) small (<1 mm) size fractions versus total zooplankton biomass. Regression lines with 95% confidence bands are based on data sets excluding the low values showing scatter (grey data points; see Table 3 for regression equations). Data are $\log_{10}$ transformed

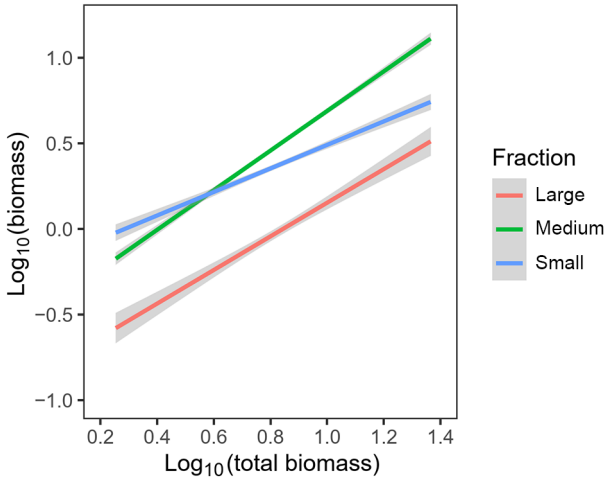

Fig. 4. Regression lines with 95% confidence bands for zooplankton biomass (g DW m^{-2}) of 3 size fractions (large: >2 mm; medium: 1–2 mm; small: <1 mm) versus total zooplankton biomass for the data set for the period 1989–2020 excluding the low values showing scatter (based on black data points in Fig. 3; regressions identified as R in Table 3)

of data points at low values, especially for the large fraction, reflecting larger methodological errors associated with the determination of low biomass. Low values are seen as statistical outliers in Fig. 2, reflecting 'inflation' of separation of data points at the low end of the log scale. We recalculated regressions excluding low values (shown as grey data points in Fig. 3). The 2 sets of regressions gave similar results (Table 3). The most noticeable difference was somewhat steeper slopes and lower intercepts of regressions with the full data set, which may be an artefact of the disproportional influence of log-transformed low data points as a downward 'pull' on the left end of the regression lines (Fig. 3).

The regression slopes for the 3 fractions were significantly different, with a steeper slope for the medium fraction (1.16) and a flatter slope for the small fraction (0.69) (Table 3, restricted data set). While the medium fraction was on average larger than the small fraction (48 vs. 35% of the total), the 2 regressions crossed at a $\log_{10}$ value of about 0.6, corresponding to a total biomass of about 4 g DW m^{-2} (Fig. 4). Above this level, the biomass of the medium fraction becomes progressively more dominant, whereas below ~4 g DW m^{-2}, the small fraction is dominant. The regressions show that moving from high to low total biomass values, there is a progressive shift for the smaller fraction becoming relatively more important. The regression slope for the large fraction was close to unity (0.98) and not statistically different from 1 (Table 3).

3.3.2. Data sets split according to depth, geographical regions, and time

Depth. Shallow polygons (<220 m depth) showed on average significantly lower biomass than deep polygons (>255 m depth) for each of the 3 fractions (Fig. S3 in the Supplement; *t*-test, $t > 4.8$, $p < 0.001$). Regressions of biomass of fractions versus total biomass showed a flatter slope for the small fraction compared to the medium and large fractions for the group of shallow polygons (Table 4; Fig. S4 in the Supplement). The regressions for small and medium fractions crossed at a $\log_{10}$ value of ~0.6 for total biomass for the shallow category (Fig. 5). There was no significant difference between the slopes for the group of deep polygons (Table 4), and the regressions for small and medium fractions did not cross in the investigated data range (Fig. 5).

Geographical regions. When the data set was broken down into 3 regions (Atlantic, Central, and Arctic), the most notable difference was lower biomass for the group of central polygons in the medium fraction (Fig. S5 in the Supplement). Based on 95% CIs, regression slopes for biomass of fractions versus total biomass were not significantly different in the Arctic and Atlantic regions (Table 4). In the central region, however, the regression slope was significantly lower (flatter) for the small fraction compared to the medium and large fractions (Table 4, Fig. 6; Fig. S6 in the Supplement). In the case of the central polygons, the regression lines for the small and medium fractions crossed at a $\log_{10}$ value of ~0.75, or ~5 g DW m^{-2} for total biomass (Fig. 6). The regression slope of the small fraction was also lower in the Arctic and Atlantic regions (although not significant at the 95% level), but the 2 regression lines for small and medium fractions did not cross for the investigated range of values (Fig. 6).

Two periods. The most noticeable difference when data were split into 2 periods (before 2007 and after) was a significantly lower biomass of the large fraction in the recent period (Fig. S7 in the Supplement; $t = 6.37$, $p < 0.001$), with the regression line for the large fraction displaced at a lower level for the recent compared to the earlier period (Fig. 7; Fig. S8 in the Supplement). A steeper slope for the medium fraction and a flatter slope for the small fraction was found in both periods, but the difference between them was more

Table 4. Results of regressions between zooplankton biomass (g DW m^{-2}) of 3 size fractions (small: <1 mm; medium: 1–2 mm; large: >2 mm) and total zooplankton biomass for polygons assigned to 2 depth categories (deep and shallow) and 3 geographic regions (Atlantic, Central, Arctic), and for 2 different time periods (older: 1989–2006; recent: 2007–2020). Log_{10}-transformed data were used in regression analyses based on data sets excluding low values (based on black data points in Fig. 3)

Regression	n	Intercept	Slope	95% CI (slope)	SE (slope)	*t* (slope)	p (slope)	R^2
				Small fraction				
Small–deep	155	−0.377	0.901	0.767–1.036	0.068	13.3	<0.001	0.54
Small–shallow	116	−0.138	0.624	0.511–0.738	0.057	10.9	<0.001	0.51
Small–Atlantic	93	−0.330	0.850	0.665–1.034	0.093	9.2	<0.001	0.48
Small–Central	93	−0.095	0.597	0.482–0.712	0.058	10.3	<0.001	0.54
Small–Arctic	47	−0.245	0.698	0.379–1.018	0.159	4.4	<0.001	0.30
Small–older	168	−0.239	0.745	0.627–0.862	0.060	12.5	<0.001	0.48
Small–recent	128	−0.149	0.617	0.507–0.728	0.056	11.1	<0.001	0.49
				Medium fraction				
Medium–deep	159	−0.355	1.039	0.953–1.126	0.044	23.8	<0.001	0.78
Medium–shallow	115	−0.485	1.153	1.041–1.264	0.056	20.5	<0.001	0.79
Medium–Atlantic	96	−0.367	1.061	0.949–1.173	0.056	18.8	<0.001	0.79
Medium–Central	91	−0.571	1.222	1.122–1.323	0.051	24.2	<0.001	0.87
Medium–Arctic	47	−0.427	1.131	0.918–1.344	0.106	10.7	<0.001	0.72
Medium–older	171	−0.402	1.056	0.973–1.139	0.042	25.1	<0.001	0.79
Medium–recent	128	−0.553	1.300	1.218–1.383	0.042	31.2	<0.001	0.89
				Large fraction				
Large–deep	157	−0.723	0.841	0.585–1.097	0.129	6.5	<0.001	0.21
Large–shallow	110	−0.932	1.145	0.921–1.370	0.113	10.1	<0.001	0.49
Large–Atlantic	96	−0.738	0.828	0.508–1.149	0.161	5.1	<0.001	0.22
Large–Central	89	−1.045	1.340	1.116–1.564	0.113	11.9	<0.001	0.62
Large–Arctic	47	−0.931	1.079	0.501–1.657	0.287	3.8	<0.001	0.24
Large–older	172	−0.768	1.001	0.823–1.178	0.090	11.1	<0.001	0.42
Large–recent	120	−0.827	0.844	0.624–1.065	0.111	7.6	<0.001	0.33

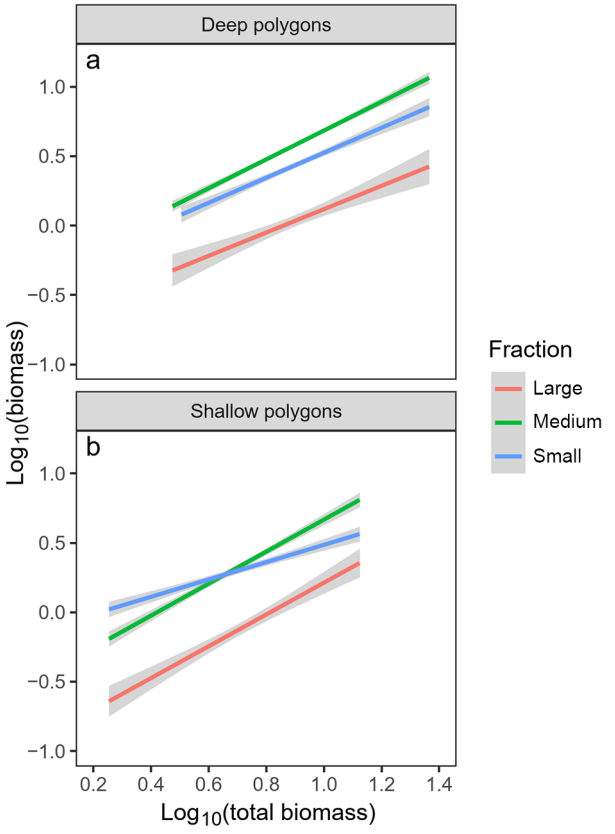

Fig. 5. Regression lines with 95% confidence bands for zooplankton biomass (g DW m^{-2}) of 3 size fractions (large: >2 mm; medium: 1–2 mm; small: <1 mm) versus total zooplankton biomass for 2 different depth categories: (a) shallow (Central Bank, Great Bank, Svalbard South, South East, North East, and Pechora) and (b) deep (Bear Island Trench, Thor Iversen Bank, Hopen Deep, South West, Southeastern Basin, and Svalbard North) polygons (see Fig. 1). Based on data sets excluding the low values showing scatter (based on black data points in Fig. 3)

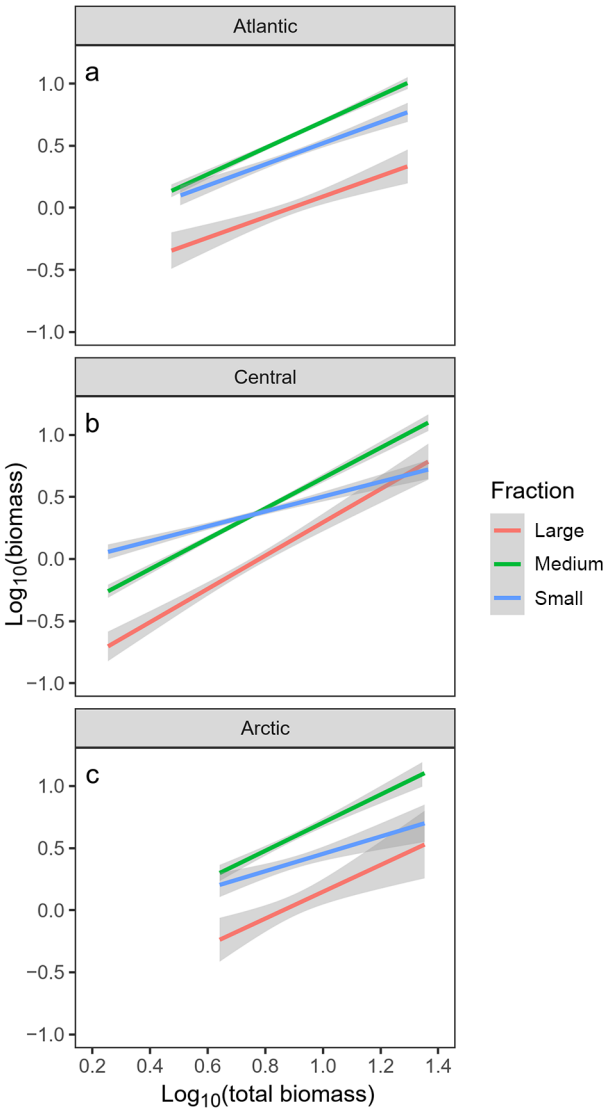

Fig. 6. Regression lines with 95% confidence bands for zooplankton biomass (g DW m^{-2}) of 3 size fractions (large: >2 mm; medium: 1–2 mm; small: <1 mm) versus total zooplankton biomass for 3 different regions: (a) Atlantic (South West, Bear Island Trench, and Thor Iversen Bank polygons); (b) central (Central Bank, Great Bank, and Hopen Deep polygons); and (c) Arctic (Franz-Victoria Trough, North East, and Svalbard North polygons) (see Fig. 1). Based on data sets excluding the low values showing scatter (based on black data points in Fig. 3)

pronounced for the recent period (Fig. 7, Table 4). Thus, the slope for the medium fraction was significantly steeper in the recent compared to the older period, while the slope of the small fraction tended to be less steep (Table 4). However, the crossing of the 2 regression lines occurred at similar total biomass values of ~4 g DW m^{-2} ($\log_{10}$ value of ~0.6) for both periods (Fig. 7).

All cases. Regression slopes were statistically significant in all cases ($p < 0.001$; Table 4), i.e. positive and different from zero. Regression slopes for the small fraction were less than unity (<1) in all cases, and statistically so (CIs not overlapping 1) in the cases of shallow and central polygons, and for both the older and recent periods (Table 4). Regression slopes for the medium fraction were >1 in all cases, and statistically significant for 3 of the same cases as for the small fraction (shallow, central, and recent period; Table 4). The regression slope was more variable for the large fraction and not statistically different from unity except for one case (central area; Table 4). We note again that the regressions are not independent (as the total is the sum of the 3 fractions), and thus the slopes of the small and medium fractions are inversely related ($r = -0.84$ for the 7 cases in Table 4).

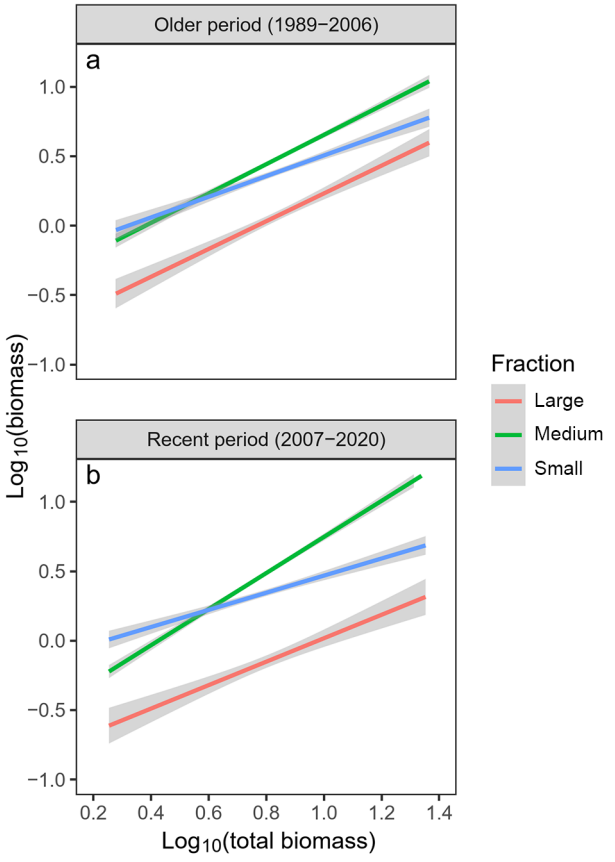

Fig. 7. Regression lines with 95% confidence bands for zooplankton biomass (g DW m^{-2}) of 3 size fractions (large: >2 mm; medium: 1–2 mm; small: <1 mm) versus total zooplankton biomass for 2 time periods: (a) older (1989–2006) and (b) recent (2007–2020). Based on data sets excluding the low values showing scatter (based on black data points in Fig. 3)

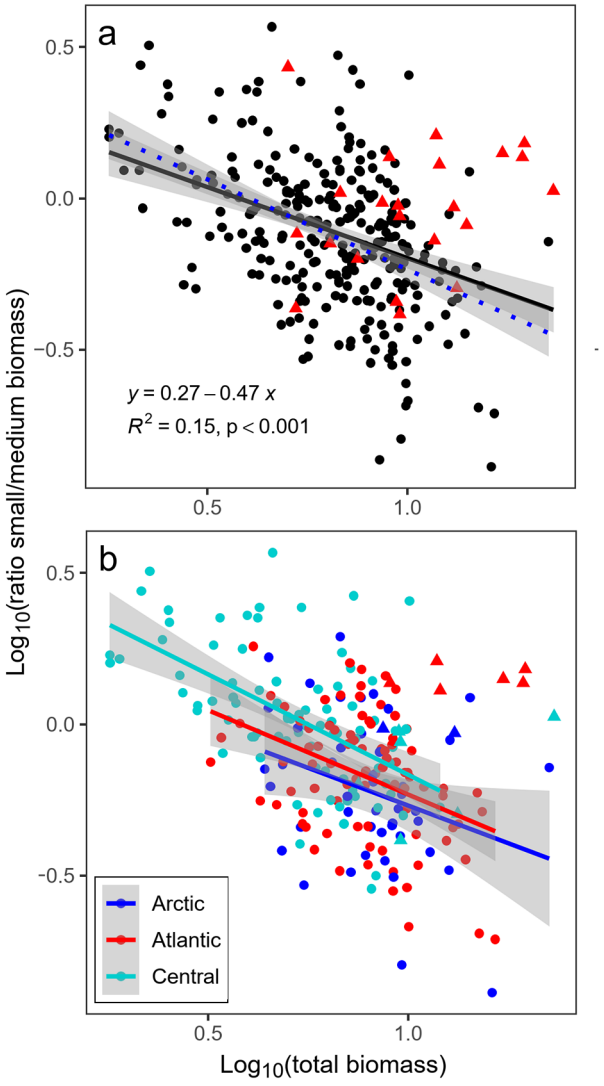

Fig. 8. Scatter plots and regression lines with 95% confidence bands for relationship between biomass ratio of the small to medium size fractions and total zooplankton biomass (both $\log_{10}$ transformed) for (a) the whole data set 1989–2020, and (b) 3 different regions: Atlantic, Central, and Arctic (see legend of Fig. 6). The black regression line with 95% confidence band in (a) is for all data points, including the red triangles which are values for 1994 and 1995 (see Section 4.3); R^2 = 0.15. The blue dotted regression line is with exclusion of the red data points, which improved the regression with R^2 = 0.22. Regression lines in (b) are based on the restricted data set (excluding low values, see Fig. 3), also excluding the years 1994 and 1995, which are the data points indicated with triangles

3.4. Ratio of biomass of the small to medium fraction

The ratio of biomass of the small to medium fraction for the individual data points (annual polygon means) showed a statistically significant decrease with increasing total biomass for the total data set (Fig. 8a), consistent with the pattern shown by the regressions for the 2 fractions separately (Fig. 4). The scatter of data points for the ratio was large, with the regression explaining 15% of the total variance (R^2 = 0.15). The regression line in Fig. 8a crosses the zero line for the log-transformed ratio at a total biomass $\log_{10}$ value of ~0.6, or ~4 g DW m^{-2}, similar to the crossing of the 2 regression lines in Fig. 4. Thus, ratios are >1 (small fraction larger than medium fraction) for total biomass of <4 g DW m^{-2} and <1 (small fraction smaller than medium fraction) for total biomass of >4 g DW m^{-2}.

The regression for the small/medium ratio can be calculated from the regression equations for the small and medium fractions separately, as given in Tables 3 & 4. This follows from the fact that the logarithm of a ratio equals the difference between the logarithms of the numerator and denominator (log small/medium

ratio = log small minus log medium). The regression slope for the ratio is the difference between the regression slopes for the small and medium fractions. For the total data set in Fig. 8a, the slope is −0.47 (for the restricted data set; −0.44 for the full data set including the low values shown as grey data points in Fig. 3). The regression slope for the small fraction was always lower than the slope for the medium fraction for the split data sets in Table 4. The regression slope for the small/medium ratio was therefore always negative, with slope values between −0.14 (deep) and −0.68 (recent period) (Figs. S9 & S10 in the Supplement). The slope was −0.21 for the Atlantic, −0.63 for the central, and −0.43 for the Arctic polygons (Fig. 8b). The lower negative slope for the Atlantic polygons was influenced by the high biomass values for 1994 and 1995 (especially for the small size fraction; see Section 4.3); removing them changed the regression slope to −0.57 (Fig. 8b).

4. DISCUSSION

4.1. Shifts in proportions among size fractions

We used linear regression to examine trends in the size composition of zooplankton biomass among the 3 size fractions. Artefacts due to random errors in the determination of biomass of the fractions are considered to be low and negligible. We see some low values for single fractions, which we consider as potentially influenced by measurement error, being inflated by log transformation at the low end of the log scale. We identified and removed such low points in some of the regressions (see Fig. 3). However, removing these low biomass points does not change the general outcome of the analyses or our interpretations and conclusions.

The regressions shown in Fig. 3 demonstrate the 'behavior' of the 'total' zooplankton compartment of the Barents Sea ecosystem, with variation spanning the zoogeographical transition from the boreal south to the Arctic north, ~3 decades of climate variability and change, and large fluctuations in the ecosystem with collapses and recoveries of the dominant capelin stock (Skjoldal 2023). Given this complexity, the consistent patterns of the zooplankton biomass fractions are remarkable. Approximately 80% of the variation in total zooplankton biomass is explained by variation in the medium size fraction through the log-linear relationship. This is even more remarkable considering the shift in dominance from *Calanus finmarchicus* to *C. glacialis*, which appears seamless in the overall biomass data set at the macroecological scale (see Section 4.2). We believe that the strict empirical relationships between the fractions and total zooplankton biomass can be of value in size-based representations and modeling of the Barents Sea and other similar high-latitude marine ecosystems.

The positive correlations among the 3 size fractions and their positive contribution to total zooplankton biomass (Tables 2 & 3) demonstrate that there is no dramatic shift in the size composition over the total range of variation in the data set. Hypothetically, if carnivorous zooplankton in the large fraction exerted strong predation pressure on zooplankton of the small fraction, inverse predator–prey oscillation might occur. This appears not to be the case. However, there are more subtle shifts in the size composition within the data set. Thus, the regression slope versus total zooplankton biomass is consistently >1 for the medium size fraction, and consistently <1 for the small size fraction (Tables 3 & 4). This translates into a negative slope of the small/medium biomass ratio with increasing total biomass (Fig. 8). The ecological implications of these trends in changes in size composition are further discussed in the following sections. The temporal (interannual) and spatial patterns in zooplankton biomass, which are behind the trends we report here, were described in more detail by Skjoldal et al. (2022b) and summarized by Skjoldal (2023).

4.2. Role of *Calanus* species

The medium size fraction made up about half of the total zooplankton biomass on average and showed a strict linear relationship with total biomass (Table 3). The 2 dominant copepods in the Barents Sea ecosystem, *C. finmarchicus* and *C. glacialis*, were estimated to contribute ~80% of the total mesozooplankton biomass (Aarflot et al. 2018, Skjoldal & Aarflot 2023). The biomass of the 2 *Calanus* species in autumn is made up mostly of copepodite stage C5, with some contribution by stage C4 and low contribution from younger copepodite stages C1–C3 (Aarflot et al. 2018, their Fig. 8). Stage C5 is contained in the medium size fraction for both *Calanus* species, while stage C4 splits about 50:50 between the medium and small fractions (Skjoldal 2021). Thus, *Calanus* is the main contributor to the medium size fraction (Skjoldal & Aarflot 2023).

Aarflot et al. (2018) found a strong linear relationship ($R^2 = 0.79$) between the biomass of *Calanus* of the 2 main species combined and total zooplankton biomass. They concluded that variation in *Calanus*

drove the overall variation in zooplankton biomass in the Barents Sea. Our results support this conclusion. It is noteworthy that the regression for *Calanus* biomass versus total biomass and the regression for the medium fraction versus total biomass found in our study were very similar, both explaining ~80% of the variance. The slopes were in both cases >1 (1.15 and 1.16, respectively), suggesting higher relative contribution by *Calanus* at high compared to low total biomass.

We note the large spatial and temporal variation in environmental conditions, ecological factors, and 'actors' at play in the ecological theater of the Barents Sea over the 3-decade span of our data. In spite of this variation, the role of the dominant *Calanus* species appears to change in a consistent and orderly way at the macroecological level, as reflected in the strict relationship with total biomass.

4.3. Shift from *Calanus* to smaller zooplankton

Associated with the strict relationship between the medium size fraction (and *Calanus*) and total zooplankton biomass, there is a clear trend of shifting dominance of the medium and small fractions across total biomass (Fig. 4). The small fraction is positively correlated with total biomass but with a flatter slope (and with less variance explained: ~50%) compared to the medium fraction (~80%). These properties result in a shift in dominance between the medium and small fractions around a total biomass value of ~4 g DW m^{-2} for the whole data set. The picture that emerges from the data is that as the total biomass decreases, driven by a decrease of the medium (*Calanus*) fraction, the biomass of the small fraction also decreases—but less so than the medium fraction. Thus, the relative importance of the small fraction in terms of biomass increases at low total biomass values (Fig. 8).

The trend of the shift from the medium to the small size fraction as total biomass declined was most pronounced for the subsets of shallow and central polygons. The 3 central polygons (Central Bank, Great Bank, and Hopen Deep) constitute the core area for the Barents Sea capelin stock (Skjoldal et al. 2022b, Skjoldal 2023). Two of these polygons (Central Bank and Great Bank) are also included in the group of shallow polygons, which showed a similar clear shift with crossing of the 2 regression lines for small and medium fractions (see Figs. 5 & 6). It thus seems that the clearest effect of a shift from the medium (*Calanus* fraction) to the small fraction is in the region with the strongest effect by capelin predation (see Section 4.5). However, the shift from the medium to the small size fraction as total biomass declined was also clearly expressed in the other regions as a general feature for the total data set.

The zooplankton biomass in 1994 and partly in 1995 was exceptional for the whole time series in showing high biomass of the small fraction driving high total biomass, most notably for the Atlantic inflow region in the southwestern Barents Sea (Skjoldal et al. 2022b, Skjoldal 2023). It is not yet clear what drove this high biomass event, but a consequence was a group of data points with high biomass of the small fraction and high total biomass, which influenced the plots of the small/medium ratio versus total biomass (Fig. 8). Calculating regressions excluding the 1994 and 1995 data resulted in steeper negative slopes for the ratio versus total biomass, with the regression for the Atlantic region becoming more similar to the regression for the central region (Fig. 8b).

4.4. Potential effects of climate change

The Barents Sea is in a warming trend and is experiencing borealization, whereby boreal species are expected to increase and expand while Arctic species are expected to decrease and retreat (Dalpadado et al. 2012, 2014, Ingvaldsen et al. 2021). Temporal trends in zooplankton biomass have been interpreted to reflect such a shift. Thus, increased biomass in the Atlantic water inflow region in the southwest and decreased biomass in the central area of the Barents Sea were explained by increased occurrence of a second generation of *C. finmarchicus* and a decline of *C. glacialis*, respectively (Skjoldal et al. 2021, 2022b, Skjoldal 2023). Both regions exhibit patterns of change in the small/medium biomass ratio, with dominance of the medium fraction in the Atlantic region and by the small fraction in the central region (Skjoldal et al. 2022b, Skjoldal 2023), consistent with the overall pattern described here.

There is a broad general inverse relationship between zooplankton body size and temperature, with larger forms associated with colder waters at high latitudes (e.g. Atkinson 1994, Angilletta et al. 2004, San Martin et al. 2006, Chiba et al. 2015, Brandão et al. 2021). Northward shifts in the distribution of zooplankton taxa have been observed associated with warming trends both in the North Atlantic and North Pacific (Beaugrand et al. 2002, Mackas et al. 2007, Richardson 2008). It is anticipated, as a broad generalization, that warming will lead to an overall reduction

in the size of zooplankton (Daufresne et al. 2009, Gardner et al. 2011). While our results are in agreement with this general pattern, the issue of change in size composition is likely complex and involves the specific species and food web interactions that operate at regional and local scales (e.g. Chiba et al. 2015, Tekwa et al. 2022).

One effect of warming on the plankton community is through phenology, or the seasonality of plankton development (Richardson 2008). In the Barents Sea, warming has caused a strong reduction in sea ice, a prolonged period with an earlier start of phytoplankton growth, and a pronounced increase in satellite-based estimates of integrated primary production (Dalpadado et al. 2020). The generational development of *C. finmarchicus* in the inflowing Atlantic water has accelerated due to higher temperatures and likely led to increased occurrence of a second summer generation (Skjoldal et al. 2021). *C. finmarchicus* typically occurs with smaller individuals in the second (summer) than in the first spring generation (Marshall et al. 1934, Wiborg 1954, McLaren et al. 2001), which is commonly ascribed as an effect of higher temperature during development of the second generation. The size reduction of the second generation is typically 5–10% in length (based on data in the references cited) and is expected to have a small effect on the size separation of biomass reported here for the autumn period. The smaller C5s and adults would still be collected in the medium fraction, and an effect would appear mainly for stage C4, which is split between the medium and small fractions. A 10% decrease in size would represent a ~10% shift of C4 biomass from the medium to the small fraction (Skjoldal 2021, using relation in his Fig. 3). With C4 making up ~25% of the biomass of *C. finmarchicus* in autumn (Aarflot et al. 2018, their Fig. 8), this change would represent a shift in the small/medium biomass ratio of ~2–3% for the contribution by *C. finmarchicus*. Such a small change would be difficult to detect.

Shifts in phenology can potentially affect the zooplankton community composition. Small copepods such as *Oithona*, *Pseudocalanus*, and *Microcalanus* species, which are contained in the small fraction (Skjoldal 2021), can have 2–3 generations per year, resulting in an increase in abundance when a second generation is developing in summer or autumn (Norrbin 1991). This may cause an increase in the biomass of the small fraction, which could lead to an increased ratio of the small to medium fraction under warmer conditions. The trends and patterns in zooplankton biomass we report here are based on a large number of ~4500 zooplankton samples. We note that for every sample, there exists a preserved and stored sample for taxonomic analysis which can be used to examine changes in species abundance and community composition. Using a smaller set of these samples with available species counts (~600 samples), the estimated biomass of small copepod species (based on numbers and average individual weights) was found to increase relative to the biomass of *Calanus* species as the total biomass of zooplankton decreased (Skjoldal & Aarflot 2023), which is consistent with the pattern for the small/medium fraction reported here.

4.5. Effects of predation

Zooplankton biomass has varied inversely with strong fluctuations of the capelin stock in the Barents Sea, which is interpreted as a top-down effect of predation by capelin (Stige et al. 2014, Dalpadado et al. 2020, Skjoldal et al. 2022b, Skjoldal 2023). Associated with declines in zooplankton biomass due to capelin predation, there have been shifts to a higher small/medium biomass ratio. Thus, the medium fraction has been dominant associated with high biomass in the inflowing Atlantic water, while the small fraction has been dominant at low biomass values in the main feeding area of capelin (Skjoldal et al. 2022b, Skjoldal 2023). These patterns, interpreted to reflect predation, are embedded as parts of the overall patterns reported here.

Capelin is a major planktivorous fish, but not the only one in the Barents Sea ecosystem. Juvenile herring of the large Norwegian spring spawning stock feed in the southern Barents Sea, while polar cod feed in the eastern and northern parts (Eriksen et al. 2017). In addition, pelagic juvenile 0-group fish of cod, haddock, and other species comprise a fourth component of pelagic planktivorous fish, distributed mainly in the western and central Barents Sea (Eriksen et al. 2011, 2017, Skjoldal et al. 2022a). These planktivores exert a predation pressure on zooplankton in addition to that caused by capelin. Much of the variation in zooplankton biomass is apparently due to the variable impact of predation by capelin and other fish predators. Thus, variation in capelin stock explained ~50% of the variance of total zooplankton biomass over the 1989–2020 data set.

There is also a large array of invertebrate predators including pelagic amphipods (*Themisto* spp.), chaetognaths, ctenophores, and small and large medusae (Swanberg & Båmstedt 1991, Dalpadado 2002, Eriksen et al. 2012). The interactions among the many fish

and invertebrate predators are expected to be complex. Thus, *Themisto* species, which are carnivores or omnivores feeding on copepods and other small prey, are themselves important prey for polar cod, capelin, and other planktivorous fish predators (Orlova et al. 2009, Eriksen et al. 2020). The abundance of *Themisto* spp. was found to vary inversely with capelin stock size, suggesting a predatory impact of capelin (Dalpadado et al. 2001). A similar predatory impact was shown for krill species as another important group of macrozooplankton in the Barents Sea (Dalpadado & Skjoldal 1996). The case of *Themisto* is an example in which an invertebrate predator is at the same time a competitor and prey for planktivorous fish (Skjoldal et al. 2004).

The positive correlation for each of the 3 size fractions with total zooplankton biomass is compatible with a dominant influence of fish predation for the variation in zooplankton biomass overall. For the large fraction, which includes invertebrate predators such as chaetognaths, hydromedusae, and amphipods (Skjoldal 2021), the biomass decreases proportionally with the biomass of the medium fraction containing *Calanus* species as the dominant herbivore component. This can be seen from the similar slopes of the regressions of the large and medium fractions versus total biomass (Tables 3 & 4). Capelin and other planktivorous fish that may target the dominant older stages of *Calanus* also eat other available large prey in the large fraction. Thus, increased predation on the medium fraction is apparently also associated with increased predation on the large fraction.

The small fraction benefits relatively, but not absolutely, as increased predation lowers the medium and large fractions and total biomass. The 1 mm screen separates copepods of median width ~0.6 mm (or prosome length ~2 mm), corresponding to the size of copepodite stage C4 *Calanus* (Skjoldal 2021). This is also the size at which planktivores such as capelin and herring start to see and eat copepods (e.g. Dalpadado et al. 2000, Dalpadado & Mowbray 2013). Therefore, the separation of the medium and small fractions corresponds broadly to the size of zooplankton that are eaten or not eaten by planktivorous fish. While the small size may protect them from fish predation, the plankton in the small fraction are prey for invertebrate predators such as chaetognaths and *Themisto* amphipods. There is likely a complex interaction between fish predation and invertebrate predators, but our results suggest that the outcome is a consistent pattern in the proportions of size fractions at a macroecological level.

5. CONCLUDING REMARKS

The extensive data set on zooplankton biomass from large-scale and long-term monitoring on autumn cruises in the Barents Sea (1989–2020) reveals a consistent and regular pattern of variation among 3 size fractions. All 3 fractions were positively related to total zooplankton biomass but with a less steep slope for the small compared to the medium and large fractions. This pattern remained consistent when the data set was split by water depth (shallow and deep), geographical areas (Atlantic, Central, Arctic), or time (before and after 2007). The medium fraction contained ~50% of the total biomass and consisted largely of the older copepodite stages of 2 biomass-dominant *Calanus* species. The small fraction contained small copepod species (mainly *Oithona* and *Pseudocalanus*) as well as young copepodites of *Calanus*. The lower slope for the small fraction was associated with an increase in the ratio of the small to medium biomass fraction with decreasing total zooplankton biomass, reflecting a shift in relative dominance from *Calanus* species to small copepods and other small forms.

The 3 size fractions showed strict relationships with total zooplankton biomass, especially the medium fraction, which explained ~80% of the variance of total biomass. These strict relationships emerge at the macroecological level from data that span a biogeographical transition from boreal to Arctic domains during more than 3 decades of climate variability and change, and with large fluctuations and changes in the ecosystem. Against this backdrop of variability and change, the strict and consistent relationships among the size fractions of zooplankton biomass are remarkable. This high degree of regularity of variability of zooplankton biomass suggests strict regulations of the zooplankton communities through density-dependent trophic interactions involving fish and invertebrate predators. How these regulations play out is a core topic for further research.

Acknowledgements. We acknowledge the good work of many scientists, technicians, officers, and crew members at IMR who contributed to the collection and analysis of the large data set on zooplankton biomass of the Barents Sea. We thank Padmini Dalpadado for preparing the data set of polygon mean values.

LITERATURE CITED

Aarflot JM, Skjoldal HR, Dalpadado P, Skern-Mauritzen M (2018) Contribution of *Calanus* species to the mesozooplankton biomass in the Barents Sea. ICES J Mar Sci 75:2342–2354

Aksnes DL, Giske J (1993) A theoretical model of aquatic visual feeding. Ecol Modell 67:233–250

Angilletta MJ Jr, Steury TD, Sears MW (2004) Temperature, growth rate, and body size in ectotherms: fitting pieces of a life-history puzzle. Integr Comp Biol 44:498–509

Atkinson D (1994) Temperature and organism size: A biological law for ectotherms? Adv Ecol Res 25:1–58

Beaugrand G, Reid PC, Ibanez F, Lindley AJ, Edwards M (2002) Reorganization of North Atlantic marine copepod biodiversity and climate. Science 296:1692–1694

Berg F, Shirajee S, Folkvord A, Godiksen JA, Skaret G, Slotte A (2021) Early life growth is affecting timing of spawning in the semelparous Barents Sea capelin (*Mallotus villosus*). Prog Oceanogr 196:102614

Brandão MC, Benedetti F, Martini S, Soviadan YD and others (2021) Macroscale patterns of oceanic zooplankton composition and size structure. Sci Rep 11:15714

Chiba S, Batten SD, Yoshiki T, Sasaki Y, Sasaoka K, Sugisaki H, Ichikawa T (2015) Temperature and zooplankton size structure: climate control and basin-scale comparison in the North Pacific. Ecol Evol 5:968–978

Conover RJ (1988) Comparative life histories in the genera *Calanus* and *Neocalanus* in high latitudes of the Northern Hemisphere. Hydrobiologia 167-168:127–142

Conover RJ, Huntley M (1991) Copepods in ice-covered seas — distribution, adaptations to seasonally limited food, metabolism, growth patterns and life cycle strategies in polar seas. J Mar Syst 2:1–41

Daase M, Falk-Petersen S, Varpe Ø, Darnis G and others (2013) Timing of reproductive events in the marine copepod *Calanus glacialis*: a pan-Arctic perspective. Can J Fish Aquat Sci 70:871–884

Dalpadado P (2002) Inter-specific variations in distribution, abundance and possible life-cycle patterns of *Themisto* spp. (Amphipoda) in the Barents Sea. Polar Biol 25:656–666

Dalpadado P, Mowbray F (2013) Comparative analysis of feeding ecology of capelin from two shelf ecosystems, off Newfoundland and in the Barents Sea. Prog Oceanogr 114:97–105

Dalpadado P, Skjoldal HR (1996) Abundance, maturity and growth of the krill species *Thysanoessa inermis* and *T. longicaudata* in the Barents Sea. Mar Ecol Prog Ser 144:175–183

Dalpadado P, Ellertsen B, Melle W, Dommasnes A (2000) Food and feeding conditions of Norwegian spring-spawning herring (*Clupea harengus*) through its feeding migrations. ICES J Mar Sci 57:843–857

Dalpadado P, Borkner N, Bogstad B, Mehl S (2001) Distribution of *Themisto* (Amphipoda) spp. in the Barents Sea and predator–prey interactions. ICES J Mar Sci 58:876–895

Dalpadado P, Ingvaldsen RB, Stige LC, Bogstad B, Knutsen T, Ottersen G, Ellertsen B (2012) Climate effects on Barents Sea ecosystem dynamics. ICES J Mar Sci 69:1303–1316

Dalpadado P, Arrigo KR, Hjøllo SS, Rey F and others (2014) Productivity in the Barents Sea — response to recent climate variability. PLOS ONE 9:e95273

Dalpadado P, Arrigo KR, van Dijken GL, Skjoldal HR and others (2020) Climate effects on temporal and spatial dynamics of phytoplankton and zooplankton in the Barents Sea. Prog Oceanogr 185:102320

Daufresne M, Lengfellner K, Sommer U (2009) Global warming benefits the small in aquatic ecosystems. Proc Natl Acad Sci USA 106:12788–12793

Eriksen E, Bogstad B, Nakken O (2011) Ecological significance of 0-group fish in the Barents Sea ecosystem. Polar Biol 34:647–657

Eriksen E, Prozorkevich D, Trofimov A, Howell D (2012) Biomass of scyphozoan jellyfish, and its spatial association with 0-group fish in the Barents Sea. PLOS ONE 7:e33050

Eriksen E, Skjoldal HR, Dolgov AV, Dalpadado P, Orlova EL, Prozorkevich DV (2016) The Barents Sea euphausiids: methodological aspects of monitoring and estimation of abundance and biomass. ICES J Mar Sci 73:1533–1544

Eriksen E, Skjoldal HR, Gjøsæter H, Primicerio R (2017) Spatial and temporal changes in the Barents Sea pelagic compartment during the recent warming. Prog Oceanogr 151:206–226

Eriksen E, Gjøsæter H, Prozorkevich D, Shamray E and others (2018) From single species surveys towards monitoring of the Barents Sea ecosystem. Prog Oceanogr 166:4–14

Eriksen E, Benzik AN, Dolgov AV, Skjoldal HR and others (2020) Diet and trophic structure of fishes in the Barents Sea: the Norwegian–Russian program 'Year of stomachs' 2015 — establishing a baseline. Prog Oceanogr 183: 102262

Falk-Petersen S, Mayzaud P, Kattner G, Sargent JR (2009) Lipids and life strategy of Arctic *Calanus.* Mar Biol Res 5:18–39

Fossheim M, Primicerio R, Johannesen E, Ingvaldsen RB, Aschan MM, Dolgov AV (2015) Recent warming leads to a rapid borealization of fish communities in the Arctic. Nat Clim Chang 5:673–677

Frainer A, Primicerio R, Kortsch S, Aune M, Dolgov AV, Fossheim M, Aschan MM (2017) Climate-driven changes in functional biogeography of Arctic marine fish communities. Proc Natl Acad Sci USA 114:12202–12207

Gardner JL, Peters A, Kearney MR, Joseph L, Heinsohn R (2011) Declining body size: A third universal response to warming? Trends Ecol Evol 26:285–291

Giske J, Skjoldal HR, Slagstad D (1998) Ecological modelling for fisheries. In: Rødseth T (ed) Models for multispecies management. Physica-Verlag, Heidelberg, p 11–68

Gjøsæter H, Bogstad B, Tjelmeland S (2009) Ecosystem effects of three capelin stock collapses in the Barents Sea. Mar Biol Res 5:40–53

Hassel A, Endresen B, Martinussen MB, Gjertsen K, Knutsen T, Johannessen ME (2020) Håndbok for forskningsgruppe Plankton. Prøvetaking og analyse. Prosedyrer for prøvetaking og pre-analyse av dyre- og planteplankton på forskningsfartøy og i laboratorium på land, version 6.0. Institute of Marine Research, Bergen

Helaouët P, Beaugrand G, Reid PC (2011) Macrophysiology of *Calanus finmarchicus* in the North Atlantic Ocean. Prog Oceanogr 91:217–228

Hop H, Gjøsæter H (2013) Polar cod (*Boreogadus saida*) and capelin (*Mallotus villosus*) as key species in marine food webs of the Arctic and the Barents Sea. Mar Biol Res 9:878–894

Hunt GL Jr, Blanchard AL, Boveng P, Dalpadado P and others (2013) The Barents and Chukchi Seas: comparison of two Arctic shelf ecosystems. J Mar Syst 109-110:43–68

Ingvaldsen RB, Assmann KM, Primicerio R, Fossheim M, Polyakov IV, Dolgov AV (2021) Physical manifestations and ecological implications of Arctic Atlantification. Nat Rev Earth Environ 2:874–889

Jakobsen T, Ozhigin VK (2011) The Barents Sea — ecosystem, resources, management. Half a century of

Russian–Norwegian cooperation. Tapir Academic Press, Trondheim
Johannesen E, Yoccoz NG, Tveraa T, Shackell NL, Ellingsen KE, Dolgov AV, Frank KT (2020) Resource-driven colonization by cod in a high Arctic food web. Ecol Evol 10:14272–14281
Kjesbu OS, Bogstad B, Devine JA, Gjøsæter H, Ingvaldsen R, Nash RDM, Skjæråsen JE (2014) Synergies between climate and management for Atlantic cod fisheries at high latitudes. Proc Natl Acad Sci USA 111:3478–3483
Kortsch S, Primicerio R, Fossheim M, Dolgov AV, Aschan M (2015) Climate change alters the structure of arctic marine food webs due to poleward shifts of boreal generalists. Proc R Soc B 282:20151546
Krysov AI, Røttingen I (2011) Herring. In: Jakobsen T, Ozhigin, VK (eds) The Barents Sea — ecosystem, resources and management. Half a century of Russian–Norwegian cooperation. Tapir Academic Press, Trondheim, p 215–224
Langbehn TJ, Varpe Ø (2017) Sea-ice loss boosts visual search: fish foraging and changing pelagic interactions in polar oceans. Glob Change Biol 23:5318–5330
Langbehn TJ, Aarflot JM, Freer J, Varpe Ø (2023) Visual predation risk and spatial distributions of large Arctic copepods along gradients of sea ice and bottom depth. Limnol Oceanogr 68:1388–1405
Lenz J (2000) Introduction. In: Harris R, Wiebe P, Lenz J, Skjoldal HR, Huntley M (eds) ICES zooplankton methodology manual. Academic Press, New York, NY, p 1–32
Longhurst AR (1985) The structure and evolution of plankton communities. Prog Oceanogr 15:1–35
Mackas DL, Batten S, Trudel M (2007) Effects on zooplankton of a warmer ocean: recent evidence from the Northeast Pacific. Prog Oceanogr 75:223–252
Marshall SM, Orr AP (1955) The biology of a marine copepod: *Calanus finmarchicus* (Gunnerus). Oliver and Boyd, Edinburgh
Marshall SM, Nicholls AG, Orr AP (1934) On the biology of *Calanus finmarchicus*. 5. Seasonal distribution, size, weight and chemical composition in Loch Striven in 1933, and their relation to phytoplankton. J Mar Biol Assoc UK 19:793–827
McLaren IA, Head E, Sameoto DD (2001) Life cycles and seasonal distributions of *Calanus finmarchicus* on the central Scotian Shelf. Can J Fish Aquat Sci 58:659–670
Melle W, Skjoldal HR (1998) Reproduction and development of *Calanus finmarchicus, C. glacialis* and *C. hyperboreus* in the Barents Sea. Mar Ecol Prog Ser 169:211–228
Melle W, Ellertsen B, Skjoldal HR (2004) Zooplankton: the link to higher trophic levels. In: Skjoldal HR, Sætre R, Færnø A, Misund OA, Røttingen I (eds) The Norwegian Sea ecosystem. Tapir Academic Press, Trondheim, p 137–202
Melle W, Runge J, Head E, Plourde S and others (2014) The North Atlantic Ocean as habitat for *Calanus finmarchicus*: environmental factors and life history traits. Prog Oceanogr 129:244–284
Norrbin MF (1991) Gonad maturation as an indication of seasonal cycles for several species of small copepods in the Barents Sea. Polar Res 10:421–432
Orlova EL, Dolgov AV, Rudneva GB, Oganin IA, Konstantinova LL (2009) Trophic relations of capelin *Mallotus villosus* and polar cod *Boreogadus saida* in the Barents Sea as a factor of impact on the ecosystem. Deep Sea Res II 56:2054–2067
Orlova EL, Dalpadado P, Knutsen T, Nesterova VN, Prokopchuk IP (2011) Zooplankton. In: Jakobsen T, Ozhigin V (eds) The Barents Sea — ecosystem, resources and management. Half a century of Russian–Norwegian cooperation. Tapir Academic Press, Trondheim, p 91–119
R Core Team (2021) R: a language and environment for statistical computing. R Foundation for Statistical Computing, Vienna
Richardson AJ (2008) In hot water: zooplankton and climate change. ICES J Mar Sci 65:279–295
Sakshaug E, Skjoldal HR (1989) Life at the ice edge. Ambio 18:60–67
San Martin E, Harris RP, Irigoien X (2006) Latitudinal variation in plankton size spectra in the Atlantic Ocean. Deep Sea Res II 53:1560–1572
Skagseth Ø, Eldevik T, Årthun M, Asbjørnsen H, Lien VS, Smedsrud LH (2020) Reduced efficiency of the Barents Sea cooling machine. Nat Clim Chang 10:661–666
Skjoldal HR (2021) Species composition of three size fractions of zooplankton used in routine monitoring of the Barents Sea ecosystem. J Plankton Res 43:762–772
Skjoldal HR (2023) Size-fractioned zooplankton biomass in the Barents Sea ecosystem: changes during four decades of warming and four capelin collapses (1980–2020). ICES J Mar Sci fsad057
Skjoldal HR, Aarflot JM (2023) Abundance and biomass of copepods and cladocerans in Atlantic and Arctic domains of the Barents Sea ecosystem. J Plankton Res 45:870–884
Skjoldal HR, Rey F (1989) Pelagic production and variability of the Barents Sea ecosystem. In: Sherman K, Alexander LM (eds) Biomass yields and geography of large marine ecosystems. AAAS Selected Symposium, No. 111. Westview Press, Boulder, CO, p 241–286
Skjoldal HR, Dalpadado P, Dommasnes A (2004) Food webs and trophic interactions. In: Skjoldal HR, Sætre R, Færnø A, Misund OA, Røttingen I (eds) The Norwegian Sea Ecosystem. Tapir Academic Press, Trondheim, p 447–506
Skjoldal HR, Wiebe PH, Postel L, Knutsen T, Kaartvedt S, Sameoto DD (2013) Intercomparison of zooplankton (net) sampling systems: results from the ICES/GLOBEC seagoing workshop. Prog Oceanogr 108:1–42
Skjoldal HR, Prokopchuk I, Bagøien E, Dalpadado P, Nesterova V, Rønning J, Knutsen T (2019) Comparison of Juday and WP2 nets used in joint Norwegian–Russian monitoring of zooplankton in the Barents Sea. J Plankton Res 41:759–769
Skjoldal HR, Aarflot JM, Bagøien E, Skagseth Ø, Rønning J, Lien VS (2021) Seasonal and interannual variability in abundance and population development of *Calanus finmarchicus* at the western entrance to the Barents Sea, 1995–2019. Prog Oceanogr 195:102574
Skjoldal HR, Eriksen E, Gjøsæter H, Skagseth Ø, Prozorkevich D, Lien VS (2022a) Recruitment variability of fish stocks in the Barents Sea: spatial and temporal variation in 0-group fish length of six commercial species during recent decades of warming (1980–2017). Prog Oceanogr 206:102845
Skjoldal HR, Eriksen E, Gjøsæter H (2022b) Size-fractioned zooplankton biomass in the Barents Sea: spatial patterns and temporal variations during three decades of warming and strong fluctuations of the capelin stock (1989–2020). Prog Oceanogr 206:102852
Stige LC, Dalpadado P, Orlova E, Boulay AC, Durant JM, Ottersen G, Stenseth NC (2014) Spatiotemporal statistical analyses reveal predator-driven zooplankton fluctuations in the Barents Sea. Prog Oceanogr 120:243–253

Stige LC, Eriksen E, Dalpadado P, Ono K (2019) Direct and indirect effects of sea ice cover on major zooplankton groups and planktivorous fishes in the Barents Sea. ICES J Mar Sci 76:i24–i36

Strand E, Bagøien E, Edwards M, Broms C, Klevjer T (2020) Spatial distributions and seasonality of four *Calanus* species in the Northeast Atlantic. Prog Oceanogr 185: 102344

Swanberg N, Båmstedt U (1991) Ctenophora in the Arctic: the abundance, distribution and predatory impact of the cydippid ctenophore *Mertensia ovum* (Fabricius) in the Barents Sea. In: Sakshaug E, Hopkins CCE, Øritsland NA (eds) Proceedings of the Pro Mare symposium on polar marine ecology, Trondheim, 12–16 May 1990. Polar Res (Spec Issue) 10:507–524

Tande K (1991) *Calanus* in North Norwegian fjords and in the Barents Sea. Polar Res 10:389–408

Tekwa EW, Watson JR, Pinsky ML (2022) Body size and food-web interactions mediate species range shifts under warming. Proc R Soc B 289:20212755

Wassmann P, Reigstad M, Haug T, Rudels B and others (2006) Food webs and carbon flux in the Barents Sea. Prog Oceanogr 71:232–287

Weydmann A, Coelho NC, Serrao EA, Burzyński A, Pearson GA (2016) Pan-Arctic population of the keystone copepod *Calanus glacialis.* Polar Biol 39:2311–2318

Wiborg KF (1954) Investigations on zooplankton in coastal and offshore waters of western and northwestern Norway with special reference to the copepods. Fiskdir Skr (Havunders) 11:1–245

Editorial responsibility: Shin-ichi Uye, Higashi-Hiroshima, Japan
Reviewed by: L. Yebra and 2 anonymous referees

Submitted: August 28, 2023
Accepted: November 7, 2023
Proofs received from author(s): January 7, 2024